Astron. Astrophys. 362, 1077–1082 (2000)

ASTRONOMY AND ASTROPHYSICS

Non-LTE analysis of neutral magnesium in cool stars⋆

G. Zhao[1,2] **and T. Gehren**[1,2]

[1] Beijing Astronomical Observatory, Chinese Academy of Sciences, 100012 Beijing, P.R. China
[2] Institut für Astronomie und Astrophysik der Universität München, Scheinerstrasse 1, 81679 München, Germany
(zg@orion.bao.ac.cn, gehren@usm.uni-muenchen.de)

Received 21 June 2000 / Accepted 31 August 2000

Abstract. Calculations of the statistical equilibrium of magnesium in the solar photosphere have shown that NLTE populations hardly affect Mg line formation in the Sun. However, in metal-poor dwarfs and giants the influence of electron collisions is reduced, and the ultraviolet radiation field, enhanced due to reduced background line opacity, results in more pronounced NLTE effects. In the photosphere of a cool star excitation and ionization due to collisions with neutral hydrogen can outweigh electron collisions. Analyses based on NLTE populations lead to significantly higher Mg abundances than those calculated from LTE. We calculate magnesium abundances in 10 cool dwarfs and subgiants with metallicities from -2.29 to 0.0. The results are based on spectra of high-resolution and high signal-to-noise ratio. Stellar effective temperatures are derived from Balmer line profiles, surface gravities from Hipparcos parallaxes and the wings of the Mg Ib triplet, and metal abundances and microturbulence velocities are obtained from LTE analyses of Fe II line profiles. For stars with metallicities between $-2.0 <$ [Fe/H] < -1.0 abundance corrections $\Delta[\mathrm{Mg/H}]_{\mathrm{NLTE-LTE}} \sim 0.05$–$0.11$ are found. As expected the corrections increase with decreasing metal abundance, and they increase slightly with decreasing surface gravity. We also calculate the statistical equilibrium of magnesium for series of model atmospheres with different stellar parameters and find that $\Delta[\mathrm{Mg/H}]_{\mathrm{NLTE-LTE}}$ increases with effective temperature between 5200 and 6500 K. For extremely metal-poor stars the abundance corrections approach $\Delta[\mathrm{Mg/H}]_{\mathrm{NLTE-LTE}} \sim 0.23$ at [Fe/H] ~ -3.0.

Key words: atomic processes – line: formation – stars: abundances – stars: late-type

1. Introduction

Abundance patterns of α-elements, such as Mg, Si and Ca, in stars with different metallicities are important for understanding the chemical evolution of Galaxy. The first stellar generations are supposed to have produced mostly α-elements during massive supernova explosions of type II. Studies of α-element synthesis in SNe II have been undertaken by Arnett (1991), Thielemann et al. (1996), Woosley & Weaver (1995), and Nakamura et al. (1999). Due to small differences in the way stellar winds and semi-convection are treated and in the specification of the *mass cut* and explosion mechanism their predictions differ, mainly in the respective Fe yields but also in the pre-explosion yields of Mg. There is no question that Mg, in principle, is less affected by the fine-tuning of SN II explosions. Therefore, inasmuch as the products of SN II nucleosynthesis are mixed into interstellar space ^{24}Mg should constitute a reliable reference of the early evolution of the Galaxy. Due to the number of strong absorption lines found in the spectra of even the metal-poor stars, Mg I is easier to observe than e.g. O I. However, it shares the disadvantage of most neutral metals in the atmospheres of moderately cool stars with Mg II being the dominant ionization stage at temperatures above 5000 K. Consequently, neutral magnesium is sensitive to deviations from *local thermodynamic equilibrium*, particularly as its ionization balance is dominated by large photoionization cross-sections from the $3\mathrm{p}\,^3\mathrm{P^o}$ state. In metal-poor stars reduced line-blanketing produces an increased UV radiation field that, in combination with the large cross-sections, leads to strong photoionization rates; this makes Mg I even more sensitive to NLTE and affects any careful abundance analysis of Mg in these objects. Moreover, the density of free electrons decreases roughly in proportion to metal abundance, and the collision rates become correspondingly smaller. Together this change of microscopic interaction processes should lead to substantially stronger deviations from LTE in metal-poor stars at optical depths $\log \tau_{\mathrm{c}}$ between -3 and 0, if the reduced electron collisional interaction is not compensated by hydrogen collisions (Baumüller & Gehren 1996, 1997).

In our present study, we use several Mg I lines chosen from the solar spectrum which were carefully analyzed previously (Zhao et al. 1998, hereafter Paper I). The standard atmospheric models we use in our present analysis are described in Sect. 2. We start with test calculations including the standard model atom of Paper I, and we fit the calculated NLTE equivalent widths for models of different stellar parameters. We determine Mg *abundance corrections* due to differences between NLTE

Send offprint requests to: G. Zhao

⋆ Based on observations collected at the German-Spanish Astronomical Center, Calar Alto, Spain and Beijing Astronomical Observatory, Xinglong, China

and LTE analyses for series of model atmospheres with the different stellar parameters in Sect. 3. All Mg I lines considered here are reproduced using standard NLTE line formation techniques with the radiative transfer solved in the Auer-Heasley scheme, taking into account the interaction processes between all levels of the Mg model atom. A previous investigation (Paper I) has demonstrated how the line profiles observed in the solar spectrum can be used to improve the atomic model of neutral magnesium. This model is the subject of further scrutiny in the light of information coming from comparison of test calculations with line profiles in the spectra of metal-poor stars. We then calculate magnesium abundances of 10 cool dwarfs and subgiants with metallicities from -2.29 to 0.0 using both LTE and NLTE line formation techniques in Sect. 4. Our conclusions are given in last section.

2. Model atmospheres

The statistical equilibrium calculations are performed in horizontally homogeneous LTE model atmospheres in hydrostatic equilibrium. We account for metallic and molecular UV line absorption using Kurucz' (1992) opacity distribution functions (ODF) interpolated for the proper stellar metallicities. In order to use the meteoritic iron abundance $\log \varepsilon_{Fe} = 7.51$ as the solar reference, we scaled Kurucz' ODF by -0.16 dex to put his iron opacity on the proper scale. Bound-free opacities were computed with solar abundances from Holweger (1979), scaled by the stellar metallicities, and in case of [Fe/H] < -0.6 corrected for a general enhancement of α-element abundances of O, Mg, and Si with [α/Fe] = 0.4. Since Mg is the most important electron donator among the α-elements this approximation follows the results found by Fuhrmann et al. (1995). Convection is taken into account parametrically with a mixing-length of 0.5 pressure scale heights (see Fuhrmann et al. 1993).

The reason for adopting this model as a standard is that we can easily use the model to calculate stellar atmospheres differentially with full physics included. On the other hand, the abundance *differences* between the LTE and NLTE calculations have nearly the same value independent of the type of model atmospheres adopted, even though we had to adjust some line parameters (e.g. logC_6, $\log gf$) in order to obtain a better line fit (*cf.* Paper I).

3. NLTE line formation

3.1. The standard atomic model

The standard atomic model we used in this analysis is basically the same as that used for the solar calculations (*cf.* Paper I). The neutral magnesium model includes all levels nℓ up to n $= 9$ and $\ell \leq \mathrm{n} - 1$ resulting in a total of 83 Mg I terms plus the doublet ground state of Mg II. All energies were taken from the compilation of Martin & Zalubas (1980) except for those terms with $\ell > 5$ which were obtained using the polarization formula of Chang & Noyes (1983). Fine structure splitting has been neglected. This model is nearly the same as that used by Carlsson et al. (1992). All terms are coupled by radiative and collisional interactions as described in more detail in Paper I.

We have shown in Paper I that collisional interaction with neutral hydrogen atoms will not affect the results obtained for the solar Mg I lines except those in the infrared. However, since neutral hydrogen collision rates do not depend on metal abundance, they can maintain an important influence in metal-poor stellar atmospheres and raise the total collision rates to high enough efficiency at which they can even compensate the strongly increased photoionization. As outlined in Paper I the hydrogen collisions are based on the formula of Drawin (1969). It is most often used in a form due to Steenbock & Holweger (1984) although the validity of this formula cannot be judged. We have used it as an order of magnitude estimate and carefully investigated the influence of hydrogen collisions on our atomic model by fitting all available Mg I lines modifying Drawin's formula by a scaling factor. For Mg I it turns out (as was the case for aluminium) that this factor should vary *exponentially* with upper level excitation energy E_{n} (in eV), $S_{\mathrm{H}} = 1000 \exp\{-\mathrm{n}E_{\mathrm{n}}/2\}$. This was determined in a fully empirical manner recomputing the complete NLTE line formation with statistical equilibrium equations including the scaled hydrogen collision rates, and it enabled us to fit solar lines of different excitation energies. The decrease of hydrogen collision cross-sections with excitation energy is also in rough agreement with Kaulakys' (1985, 1986) prediction for Rydberg transitions.

3.2. Statistical equilibrium calculations for different stellar parameters

The statistical equilibrium is calculated using the DETAIL code (Giddings 1981; Butler & Giddings 1985) in a version based on the method of complete linearization as described by Auer & Heasley (1976). The calculation includes all radiative line transitions, most of them represented by Doppler profiles; 99 lines were linearized. The Mg b lines are treated with full radiative and van der Waals damping. The linearized line transitions were selected from test calculations including different combinations with a preference for the stronger transitions including the $\ell = \mathrm{n} - 1$ levels. Adding more transitions did not change the results. The bound-free transitions of the lowest 22 levels were linearized, too.

In a star such as the Sun the flux in the ultraviolet spectral region is determined to a large part by opacities due to metal line absorption. As in our analysis of the solar Mg spectrum we use the opacity distribution functions of Kurucz (1992) to represent this opacity. In these ODF data single line opacities in small frequency intervals are represented by superlines; consequently, the ODF opacity is not identical to that required at a specific position in frequency space. For the calculation of a model atmosphere this simplification is a sufficient approximation, but for NLTE line formation the actual radiation field across a line transition or an ionization continuum is important for the determination of the statistical equilibrium of an atom. For bound-free transitions the exact position of the absorbing lines is less important, and the use of the ODFs will be reli-

Table 1. Abundance differences between NLTE and LTE obtained by fitting calculated LTE equivalent widths of Mg I lines using the same parameters for various stellar model atmospheres based on our line-blanketed model grid. Results refer to Δ[Mg/H] = [Mg/H]$_{\rm NLTE}$ - [Mg/H]$_{\rm LTE}$

$T_{\rm eff}$	$\log g$	[Fe/H]	4571Å	4703Å	4730Å	5528Å	5711Å	7657Å	8806Å	8213Å	11828Å	$\overline{\Delta[Mg/H]} \pm \sigma$
5200	4.50	0.0	0.022	0.014	0.021	0.010	0.015	0.035	0.001	0.042	0.004	0.018±0.014
5200	4.50	-1.0	0.060	0.038	0.051	0.022	0.045	0.065	0.019	0.115	0.025	0.049±0.030
5200	4.50	-2.0	0.091	0.039	0.058	0.028	0.052	0.055	0.045	0.098	0.045	0.057±0.023
5200	4.50	-3.0	0.113	0.062	0.068	0.058	0.060	0.050	0.075	0.095	0.075	0.073±0.020
5780	4.44	0.0	0.047	0.028	0.042	0.023	0.050	0.060	0.004	0.076	0.019	0.039±0.022
5780	4.44	-1.0	0.087	0.073	0.088	0.060	0.104	0.130	0.041	0.202	0.050	0.093±0.049
5780	4.44	-2.0	0.128	0.123	0.111	0.099	0.117	0.120	0.079	0.234	0.090	0.122±0.045
5780	4.44	-3.0	0.182	0.190	0.172	0.180	0.172	0.200	0.163	0.430	0.157	0.205±0.085
5780	3.50	0.0	0.060	0.033	0.062	0.028	0.090	0.115	0.016	0.095	0.026	0.058±0.035
5780	3.50	-1.0	0.101	0.081	0.120	0.054	0.151	0.180	0.018	0.252	0.053	0.112±0.073
5780	3.50	-2.0	0.147	0.157	0.137	0.118	0.136	0.120	0.045	0.264	0.085	0.134±0.060
5780	3.50	-3.0	0.201	0.224	0.206	0.211	0.207	0.210	0.212	0.429	0.210	0.234±0.073
6500	4.50	0.0	0.042	0.041	0.046	0.045	0.083	0.100	0.042	0.095	0.047	0.060±0.025
6500	4.50	-1.0	0.077	0.102	0.088	0.090	0.123	0.150	0.051	0.188	0.072	0.105±0.043
6500	4.50	-2.0	0.096	0.142	0.101	0.120	0.105	0.120	0.075	0.178	0.094	0.115±0.031
6500	4.50	-3.0	0.148	0.178	0.162	0.182	0.179	0.200	0.178	0.302	0.175	0.189±0.045

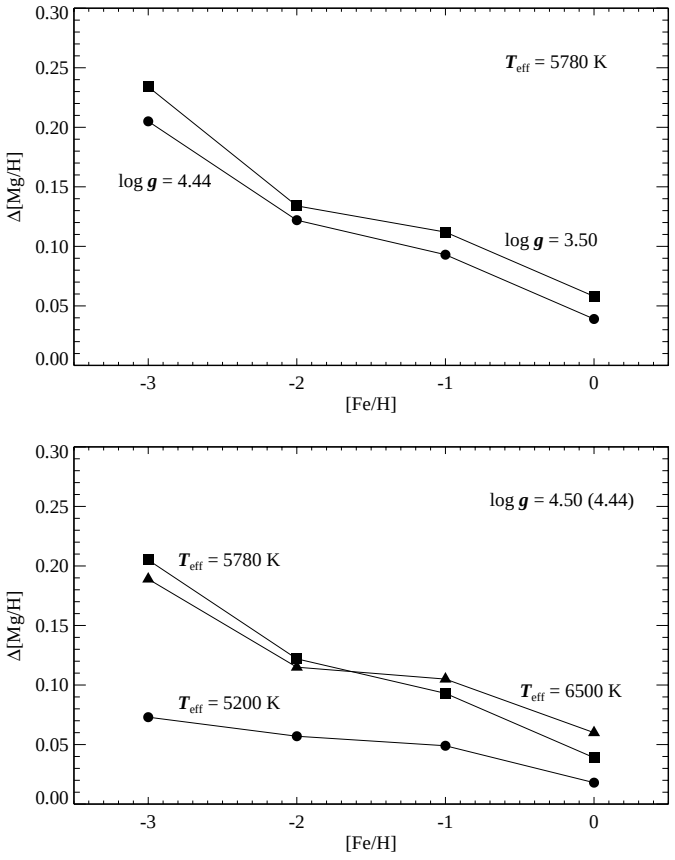

Fig. 1. NLTE corrections of the magnesium abundances versus [Fe/H] for the model grids, where Δ[Mg/H] = [Mg/H]$_{\rm NLTE}$ − [Mg/H]$_{\rm LTE}$. Top: $T_{\rm eff}$ = 5780 K, $\log g$ = 3.50 and 4.44. Bottom: $\log g$ = 4.50 (4.44 for $T_{\rm eff}$ = 5780 K), $T_{\rm eff}$ = 5200, 5780, and 6500 K.

able, provided the intervals are small enough in the frequency region near the ionization edge. For a bound-bound transition with its narrow line width it can be important in which part of the broad synthetic ODF line it is formed. We include the additional ODF opacity in the UV for wavelengths between 1300 and 3860 Å to allow for a realistic behaviour of the ionization from the ground state and the first excited level without affecting most of the line transitions. Only a few Mg I lines are found in this region allowing us to omit additional line opacities as most of these transitions are of minor importance for the statistical equilibrium.

We use the statistical equilibrium of Mg I with hydrogen collisions from Drawin's formula (Drawin 1969) but scaled exponentially with upper level excitation energy as described in Sect. 3.1. Abundance differences between the NLTE and LTE calculations with various stellar models are shown in Table 1. These results are obtained requiring NLTE and LTE line formation to fit the same equivalent width. The results confirm that deviations of the Mg I level populations from LTE increase with decreasing metal abundance. The NLTE effects in solar metallicity stars are almost negligible. In Fig. 1 we demonstrate the variation of the NLTE corrections of magnesium abundances versus [Fe/H] for sequences of model grids with constant surface gravity, $\log g \sim 4.5$, and $T_{\rm eff} = 5200, 5780$ and 6500 K, and with constant effective temperature, $T_{\rm eff} = 5780$ K, and $\log g = 3.5$ and 4.44. From these plots it is evident that the NLTE effects are systematically stronger for the hotter models, which is in accordance with the statistical equilibrium of aluminium and sodium (Baumüller & Gehren 1996; Baumüller et al. 1998). The dependence upon temperature is, however, strongly tied to the change in ionization; as soon as $T_{\rm eff}$ drops below 5300 K, Mg II starts to recombine, and Mg I becomes more dominant. For stars at the turnoff the temperature dependence is negligible. As expected, the strongest departures from LTE are found

for models with high temperature and low metallicity. The reduction of surface gravity results in a decreased efficiency of collisions by electron and hydrogen atoms which again leads to slightly stronger NLTE effects.

4. Magnesium abundances in cool stars

Our present study is based on spectroscopic data obtained by K. Fuhrmann and M. Pfeiffer using the fiber optics cassegrain echelle spectrograph (FOCES) fed by the 2.2m telescope at the Calar Alto Observatory during three observing runs in September 1995, October 1996 and May 1997. The 1995 spectra were exposed to a 1024 $\times$ 1024 24 μ CCD, and the resolving power was $\sim$ 35,000. In October 1996 and May 1997 a 2048 $\times$ 2048 15 μ CCD was employed at R $\sim$ 60,000. Almost all the stars were observed at least twice with the signal-to-noise ratio of about 200 (Fuhrmann 1998). Details with respect to the FOCES spectrograph can be found in Pfeiffer et al. (1998). For HD 19445, HD 95128, HD 103095, HD 194598, and HD 201891 additional spectra were obtained by G. Zhao and H. Zhang with the Coudé Echelle Spectrograph attached to the 2.16 meter telescope at Beijing Astronomical Observatory (Xinglong, China) in October 1996 and March 1997. The detector is a Tek CCD (1024$\times$1024 pixels of 24 μm^2 each). The Coudé Echelle Spectrograph has two beams: a blue path and a red path. For the blue path, the 79 grooves/mm echelle grating is used along with the prism as cross-disperser and a 0.5 mm slit, leading to a resolving power of the order of 44,000. For the red path, the 31.6 grooves/mm echelle grating is used along with the prism as cross-disperser and a 0.5 mm slit, leading to a resolving power of the order of 37,000. The more detailed technique and performance descriptions of the Coudé Echelle Spectrograph can be found in the paper of Jiang (1996).

The effective temperatures of our program stars were determined from the wings of the Balmer lines H_α and H_β profile fitting. For metal-poor stars, H_γ and H_δ are also taken into account (*cf.* Fuhrmann 1998). Fortunately, the dependence of the results on effective temperature is not important for most of the stars; only HD 6582 and HD 103095 are cool enough to be affected (see Fig. 1). Surface gravities have been derived from Hipparcos data using the method given by Nissen et al. (1997). The final surface gravities are determined by comparison to the strong line wings of the Mg Ib triplet which gives a slightly higher value than that from the determination of Hipparcos data. The [Fe/H] values were adopted from the determination of Fe II lines which are insensitive to NLTE effects (Thévenin & Idiart 1999). The mircoturbulence velocity ξ_t was estimated using an extended set of Fe lines.

We note that only a few Mg I lines show a suitable line profile for spectrum synthesis in our spectra of sample stars. Therefore, four lines, namely $\lambda\lambda$ 4571, 4703, 5528 and 5711 Å, which are often used for magnesium abundance determinations are selected in our present analysis. Synthetic spectra using either LTE or NLTE level populations were calculated using the line data given in Paper I. The final results are presented in Table 2, where both the NLTE and the LTE line profile fit abundances are listed for comparison. We present the magnesium abundances of 10 cool dwarfs and subgiants using NLTE and LTE line formation in Fig. 2; the plots of the NLTE correction Δ[Mg/Fe] versus [Fe/H] and $\log g$ are shown, too. One of the most striking results is the difference between NLTE and LTE abundances in the very metal-poor subgiant HD 140283 and subdwarf HD 19445, corresponding to factors of 1.35 and 1.39, respectively. It is again evident how NLTE abundance correc-

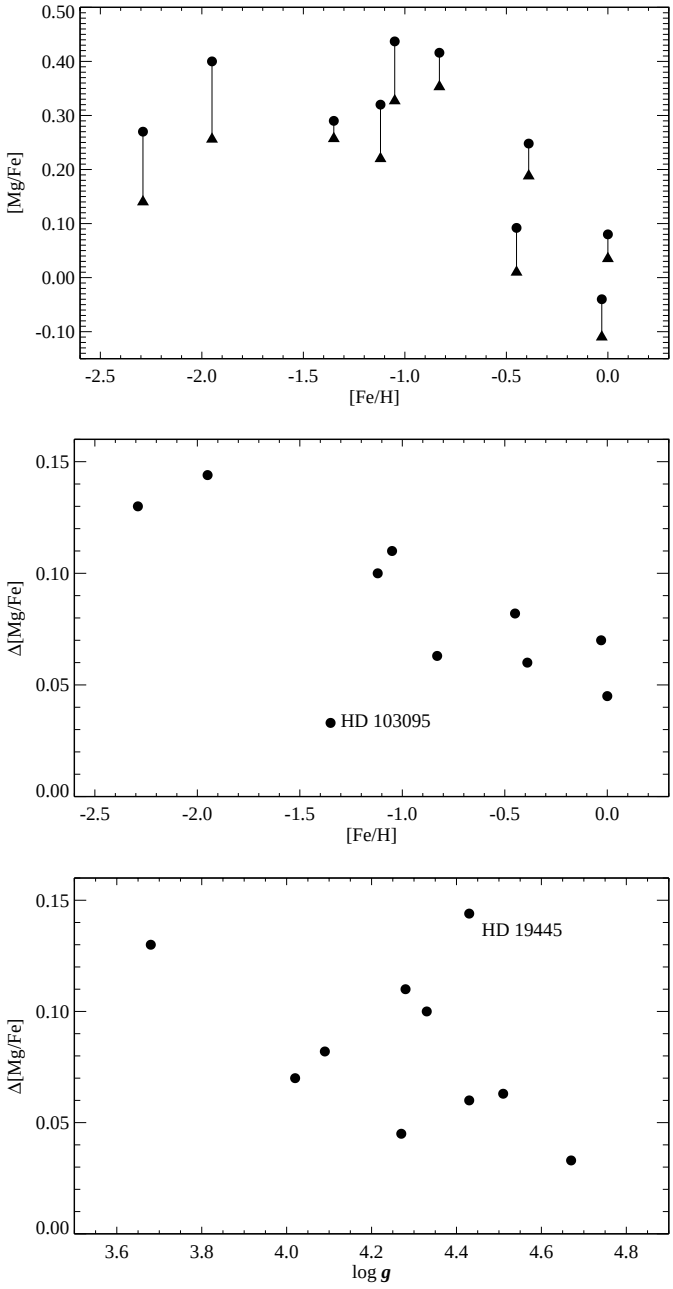

Fig. 2. Top: Magnesium abundances of 10 cool dwarfs and subgiants from NLTE and LTE line formation. The symbols of triangle and filled circle represent the LTE and NLTE results, respectively. NLTE corrections Δ[Mg/Fe] of the 10 program stars versus [Fe/H], where Δ[Mg/Fe] = $[\mathrm{Mg/Fe}]_{\mathrm{NLTE}}$ - $[\mathrm{Mg/Fe}]_{\mathrm{LTE}}$ as a function of metal abundance (middle) and surface gravity (bottom)

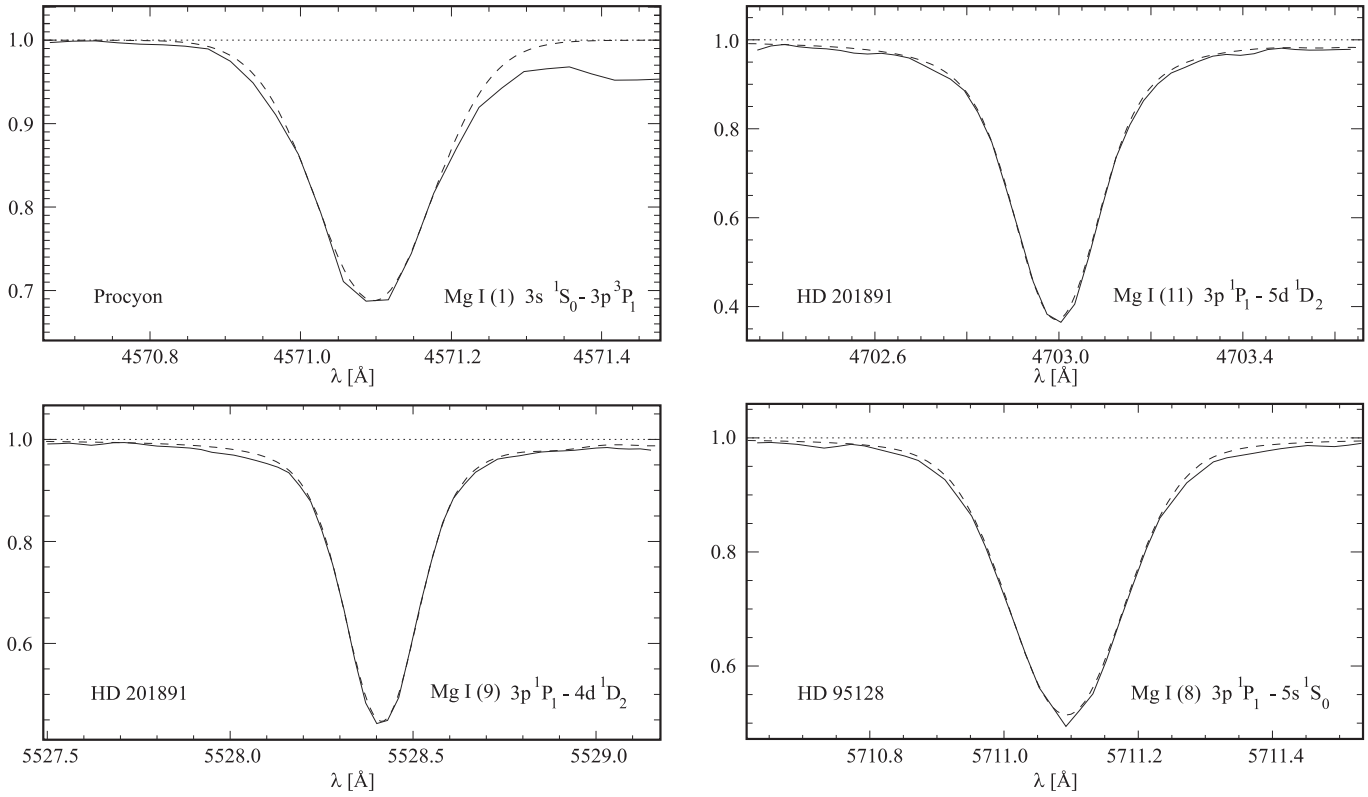

Fig. 3. Synthetic flux profiles of selected Mg I lines (dashed) compared with the observed spectra of program stars (continuous). The synthetic line profiles refer to NLTE with hydrogen collisions scaled exponentially with excitation energy. (*top left*): intercombination line $3s\,^1S - 3p\,^3P^o$ at 4571 Å. (*top right*): excited line $3p\,^1P^o - 5d\,^1D$ transition at 4703 Å. (*bottom left*): excited line $3p\,^1P^o - 4d\,^1D$ transition at 5528 Å. (*bottom right*): excited line $3p\,^1P^o - 5s\,^1S$ transition at 5711 Å.

Table 2. Stellar parameters and magnesium abundances [Mg/Fe] calculated with LTE and NLTE line formation

Object	V	$T_{\rm eff}$	$\log g$	[Fe/H]	ξ_t	4571 Å		4703 Å		5528 Å		5711 Å	
HD	[mag]	[K]			[km s^{-1}]	LTE	NLTE	LTE	NLTE	LTE	NLTE	LTE	NLTE
6582	5.16	5387	4.51	–0.83	0.89	-	-	0.33	0.39	0.36	0.43	0.37	0.43
19445	8.06	6016	4.43	–1.95	1.35	0.38	0.48	0.13	0.36	0.26	0.36	-	-
30743	6.26	6298	4.09	–0.45	1.64	–0.02	0.04	-	-	0.07	0.14	–0.02	0.10
61421	0.37	6470	4.02	–0.03	1.95	–0.19	–0.14	-	-	–0.01	0.03	–0.13	–0.01
95128	5.05	5892	4.27	–0.00	1.01	-	-	-	-	0.02	0.04	0.05	0.12
103095	6.45	5110	4.67	–1.35	0.85	0.21	0.27	0.26	0.28	0.31	0.32	0.25	0.29
140283	7.21	5810	3.68	–2.29	1.49	-	-	-	-	0.14	0.27	-	-
165401	6.81	5811	4.43	–0.39	1.10	0.17	0.23	0.17	0.23	0.23	0.27	0.18	0.26
194598	8.34	6058	4.33	–1.12	1.45	0.25	0.33	0.20	0.32	0.24	0.32	0.19	0.31
201891	7.37	5943	4.28	–1.05	1.18	-	-	0.31	0.43	0.38	0.45	0.29	0.43

tions increase with decreasing stellar metallicity. There is one star HD 103095 (Groombridge 1830) that shows a different behaviour in Fig. 2 (middle); due to its low effective temperature ($\sim$ 5110 K, the lowest one in our sample stars) its ionization equilibrium is more affected by temperature than by NLTE effects. This is in accordance with our analysis for the grids of the model atmospheres in Sect. 3. The effective temperature, surface gravity, metallicity and microturbulence have typical error of $\Delta T_{\rm eff} \sim 80$ K, $\Delta \log g \sim 0.1$ dex, Δ[Fe/H] ~ 0.07 dex and $\Delta\xi_t \sim 0.2$ km s^{-1}. Consequently, the error estimate for the magnesium over hydrogen abundances is about 0.07 dex. These error estimations are nearly the same for LTE and NLTE abundance determination. Note that in most cases the abundance differences are well above the observational errors. On the other hand, the NLTE abundances based on various line profile fits generally produce a satisfactory smaller standard deviation than that of LTE abundances. This result is perhaps the most important because it shows that with high resolution ($R > 40000$), high signal-to-noise spectra it is possible to reproduce line profiles with very high accuracy. A few profile fits for the different magnesium lines are given in Fig. 3 to show the quality of the

line synthesis. They are representative for the average fit quality obtained for the $R \sim 40000$ and 60000 spectra.

5. Conclusions

The variation of [Mg/Fe] with the stellar mean metallicity [Fe/H] contains information about the chemical evolution of the Milky Way. Previous investigations of magnesium based on LTE analyses by a number of researchers (e.g. Magain 1987; Hartmann & Gehren 1988; Fuhrmann et al. 1995; Fuhrmann 1998) show that magnesium has a solar abundance ratio in disk stars ([Fe/H] ≥ -0.5), and then [Mg/Fe] becomes constant at +0.3 ... 0.4 in metal-poor stars ([Fe/H] ≤ -0.5). As shown by Fuhrmann (1998), this overabundance is a distinct result of population membership. Our new results based on the NLTE analysis of 10 cool unevolved stars demonstrate that the magnesium overabundance with respect to iron becomes even larger by roughly 0.1 dex for stars with reduced stellar metal abundance [Fe/H] due to photoionization dominating over collisions. The reduction of the surface gravity results in a decreased efficiency of collisions by electron and hydrogen atoms which also leads to small NLTE effects. The strongest departures from LTE are found for metal-poor stars with high temperature and low gravity, i.e. *turnoff* stars.

Fortunately, the trend obtained from LTE abundance analyses of magnesium in cool stars (Fuhrmann 1998) is confirmed. The significant [Mg/Fe] ratio in metal-poor stars is found from NLTE spectrum analyses, with the increased level indicating a shift to even higher stellar masses in the parent population (III). Such a trend was also found by Fuhrmann et al. (1995) or Audouze & Silk (1995) who investigated the initial mass function based on the α-element enrichment of population II. Recent investigations of the Fe II/Fe I equilibrium (see Thévenin & Idiart 1999), however, seem to demonstrate that [Mg/Fe] may be more affected by deviations from LTE when using Fe I lines to derive iron abundances. We recall that in our analysis we used only Fe II lines which are insensitive to NLTE effects.

In order to confirm the present results for magnesium, and in particular the mean abundance differences between LTE and NLTE it is necessary to reinvestigate a larger sample of stars with various metallicities based on the NLTE analysis, especially for the metal-poor stars of the thick disk and halo. Such an investigation should, however, include an Fe I NLTE analysis. Then it will be an important step improving our present understanding of stellar nucleosynthesis and the chemical evolution of the Galaxy.

Acknowledgements. This research was supported by the Deutsche Forschungsgemeinschaft, the National Natural Science Foundation of China, and the Major State Basic Research Development Program of China. We thank Dr. Klaus Fuhrmann who kindly provided the spectra data of the program stars. We thank Dr. Johannes Reetz for supporting the line synthesis code.

References

Arnett D., 1991, In: Frontiers of Stellar Evolution, ASP Conf. Ser. 20, p. 389
Audouze J., Silk J., 1995, ApJ 451, L49
Auer L.H., Heasley J.N., 1976, ApJ 205, 165
Baumüller D., Gehren T., 1996, A&A 307, 961
Baumüller D., Gehren T., 1997, A&A 325, 1088
Baumüller D., Butler K., Gehren T., 1998, A&A 338, 637
Butler K., Giddings J., 1985, Newsletter on the Analysis of Astronomical Spectra No. 9, University of London
Carlsson M., Rutten R.J., Shchukina N.G., 1992, A&A 253, 567
Chang E.S., Noyes R.W., 1983, ApJ 275, L11
Drawin H.W., 1969, Z. Physik 225, 470
Fuhrmann K., 1998, A&A 338, 161
Fuhrmann K., Axer M., Gehren T., 1993, A&A 271, 451
Fuhrmann K., Axer M., Gehren T., 1995, A&A 301, 492
Hartmann K., Gehren G., 1988, A&A 199, 269
Holweger H., 1979, In: Les Eléments et leurs Isotopes dans l'Univers. 22^{nd} Liège Symp., Liège, p. 117
Giddings J.R., 1981, Ph.D. Thesis, University of London
Jiang S.Y., 1996, In: Kaifu N. (ed.) Ground-based Astronomy in Asia. National Astronomical Observatory of Japan, p. 335
Kaulakys B., 1985, J. Phys. B 18, L167
Kaulakys B., 1986, Sov. Phys. JEPT, 64, 229
Kurucz R.L., 1992, Rev. Mex. Astron. Astrofis. 23, 181
Magain P., 1987, A&A 179, 176
Martin W.C., Zalubas R., 1980, J. Phys. Chem. Ref. Data 9, 1
Nakamura T., Umeda H., Nomoto K., et al., 1999, ApJ 517, 193
Nissen P.E., Hoeg E., Schuster W.J., 1997, In: Battrick B. (ed.) Proc. Hipparcos Venice Symp. ESA SP-402, p. 225
Pfeiffer M.J., Frank C., Baumüller D., Fuhrmann K., Gehren T., 1998, A&AS 130, 381
Steenbock W., Holweger H., 1984, A&A 130, 319
Thévenin F., Idiart T.P., 1999, ApJ 521, 753
Thielemann K.F., Nomoto K., Hashimoto M., 1996, ApJ 460, 408
Woosley S.E., Weaver T.A., 1995, ApJS 101, 181
Zhao G., Butler K., Gehren T., 1998, A&A 333, 219